We want to thank the reviewers for their support of the paper and their helpful comments and suggestions which have helped to improve our manuscript. We provide a point by point response to review.

Response to Anonymous Referee #2

In this study, Kolmogorov-Zurbenko (KZ) filter was used to decompose the time series of PM2.5 and chemical species into intra-day, diurnal, synoptic, and baseline temporal scale components (TS components), which might be helpful for a better understanding of source apportionment. However, I did not see good evaluation criteria to judge whether this relatively new approach is superior to the ME-2 or PMF without KZ. For the KZ method, different solution can be used, but it is still very questionable which solution is the best one. Therefore, I strongly suggest the authors extend the discussion to address my concern before a publication in ACP. In general, I think the author should use PMF instead of PCA for the source apportionment. In NCP, haze episode is much more frequent in winter than in summer, so the authors should use or include the winter data set for a typical application for this new approach. I agreed with the other reviewer that the overall source apportionment result is not good enough to separate different sources. Therefore, seasonal variations should be included. I would like to see diurnal variations for traffic sources and other sources as well.

Response: a) This work aims to the influence of different temporal-scale components on source contributions using Kolmogorov-Zurbenko (KZ) filter method and receptor model rather than establishes the new approach and compares it with PMF/ME2. We found that primary source impact levels mainly determined by baseline TS component (source emissions), and secondary source impact levels were mainly influenced by synoptic and baseline TS component (synoptic scale weather fluctuations and source emissions).

b) We reanalyzed a new dataset (about 5 months) that collected in Tianjin, China to strongly support our findings.

We collected dataset during winter in Tianjin, China and analyzed the dataset following the same process of Beijing dataset. Results from Tianjin datasets shown that diurnal and synoptic TS components had higher relative contributions to the total variance of OC, EC, $PM_{2.5}$, and most ions and elements than the intra-day and baseline TS components. Six source categories were identified using ME-2 from both original and RD datasets in Tianjin, including crustal dust, vehicle emissions, coal combustion, secondary formation, biomass burning & sea salt, and industrial source. While industrial source has not been identified from both RD and RS dataset that mixed with crustal dust. The TPS impacts calculated from the original, RI, RD, and RS datasets were similar (ranged from 33.8 to 38.2 μg m^{-3}), the TSS impacts derived from the original and RI datasets exhibited similar source impacts (about 33 μg m^{-3}), which was higher than the solution from the RD (27.3 μg m^{-3}) and RS dataset (23.0 μg m^{-3}). Both Beijing and Tianjin results suggested TPS impact levels were mainly influenced by baseline TS component, and TSS impact levels were mainly influenced by synoptic and baseline TS components. Seasonal variations of source impacts were investigated in Tianjin. A more significant decrease in secondary source impact during winter suggested that the synoptic TS component had a more significant impact on the secondary source during winter than during the fall in this work.

Detailed discussion as follow:

Long-Term observations were conducted in Tianjin, China, from October 03, 2017 to March 16, 2018. $PM_{2.5}$, inorganic ions, OC/EC, and heavy metals were measured by

β-ray monitor, an ambient ion monitor (AIM, URG 9000D, URG Corporation, USA) (Shi et al., 2017), OC/EC analyzer (OCEC-100, Focused Photonics Inc, China) and a continuous atmospheric heavy metals monitoring system (AMMS-100, Focused Photonics Inc, China) (Ye et al., 2012), respectively. Twenty chemical species at 1 h time resolution were selected for analysis, including NH_4^+, Na^+, Mg^{2+}, K^+, Cl^-, NO_3^-, SO_4^{2-}, As, Ca, Tl, Br, Cs, Pb, Se, Cr, Zn, Fe, Mn, OC, and EC. Other species were excluded since they contained more than 40% values below the detection limit.

Each TS component contribution to the total variance of $PM_{2.5}$ and the chemical species concentrations in Tianjin was listed in Table S7. For $PM_{2.5}$, OC, EC, and inorganic ions (except Mg^{2+} and Na^+), the diurnal and synoptic TS components had higher relative contributions to the total variance of these species than the intra-day and baseline TS components. Baseline TS component had largest relative contributions to the total variance of Ca, followed by the intra-day, intra-day, and diurnal TS components. For other elements (except Tl and Br), diurnal and synoptic/intra-day TS components had the larger amplitudes and were the larger contributors to the total variance of the concentrations. Dataset observed in Tianjin was processed following the 2.4 section to create RI, RD, RS, RBL datasets. For $PM_{2.5}$ and all chemical species, the largest average concentrations decline occurred when removed baseline TS component from original dataset (Table S8), suggesting baseline TS components dominating the average concentrations of $PM_{2.5}$ and chemical species.

The original, RI, RD, and RS datasets were respectively introduced into ME-2 to identify the sources of $PM_{2.5}$ (Figures 5 and 6). The regression analysis for the modeled and measured species mass concentrations shown that the slopes and r values of $PM_{2.5}$

were ranged from 0.65 to 0.87 and 0.80 to 0.94, respectively (Figure S13). Performance of solutions from RI and BL datasets are better than the solution from the original dataset, due to slops and r values were closer to 1 than the corresponding results from the original dataset. Comparable performance was obtained from RD, RS, and Original datasets. Six source categories were identified using ME-2 from both original and RD datasets, including crustal dust, vehicle emissions, coal combustion, secondary formation, biomass burning & sea salt, and industrial source. Biomass burning & sea salt was characterized by K^+ and Cl^- (Tian et al., 2018; Zhu et al., 2018). The industrial source has high loadings of Zn (Monsalve et al., 2018; Ojekunle et al., 2018). While five sources were obtained from both RD and RS dataset except industrial source that mixed with crustal dust. Crustal dust & industrial source was identified by Ca, Fe, and Zn. We tried to separate the crustal dust and indusial source by adding factor number. However, the adding factor did not has a noticeable characteristic of factor profile and cannot be explained by crustal dust or indusial source. For Tianjin dataset, crustal dust was identified and mixed with the industrial source for the RD and RS datasets, suggesting removing diurnal or synoptic TS component affects source identification. Nitrate and sulfate did not separate from each other after removing the synoptic TS component, because they have similar variation trend. The correlation was 0.70 for the RS dataset, which is close to the results of other datasets (0.80, 0.81, and 0.84 in the original, RI, and RD datasets, respectively).

The correlation coefficient of the time series of source impacts between the original and the RI, RD, and RS datasets was listed in Table S9. Synoptic TS component

mainly influences secondary formation impact variation due to a relative low correlation of temporal trend between original and RS datasets. Other four sources, including crustal dust, vehicle emissions, coal combustion, and biomass burning & sea salt, are mainly affected by diurnal and synoptic scale influences. The average impacts of individual source categories on $PM_{2.5}$ from the datasets with removed TS components (Table 4). Vehicle emissions, crustal dust, coal combustion, biomass burning & sea salt, and indusial source were combined for the TPS. For the entire sampling period, the impacts of TPS obtained from the original, RI, RD, and RS datasets were similar to each other, ranging from 33.8 to 38.2 μg m^{-3}. The TSS (secondary formation) solutions from the original and RI datasets exhibited similar source impacts, accounting for about 33 μg m^{-3}, which was higher than the solution from the RD (27.3 μg m^{-3}) and RS dataset (23.0 μg m^{-3}). The RBL dataset, including about 45% negative values, was analyzed by PCA (Table S10). Four factors, including crustal dust (44.9%), secondary formation (8.7%), industrial source & coal combustion (6.4%), and vehicle (5.4%), were extracted and accounted for 65.4% of the total variance. In additional, ME-2 was applied to the baseline dataset and identified crustal dust, vehicle emissions, coal combustion, and secondary formation (Figure S14 and Table S11). The average TPS and TSS impacts on $PM_{2.5}$ mass concentrations were 29.6 μg m^{-3} (58%) and 21.3 μg m^{-3} (42%) respectively.

Seasonal variations of source impacts were investigated in Tianjin, as shown in Table 4. Winter period in this work included 15 days in March 2018 because 15 days is too short to present spring. The TPS impacts derived from the original, RI, RD, and RS

datasets were relatively stable, ranging from 31.9 to 35.8μg m^{-3} during fall and 33.6 to 37.1 μg m^{-3} during winter (Table 4). The TSS impacts decreased from 27.6 (original dataset) to 20.5μg m^{-3} (RS dataset) during the fall and from 39.0 (original dataset) to 26.6μg m^{-3} (RS dataset) during winter. A more significant decrease in secondary source impact during winter suggested that the synoptic TS component had a more significant impact on the secondary source during winter than during the fall in this work.

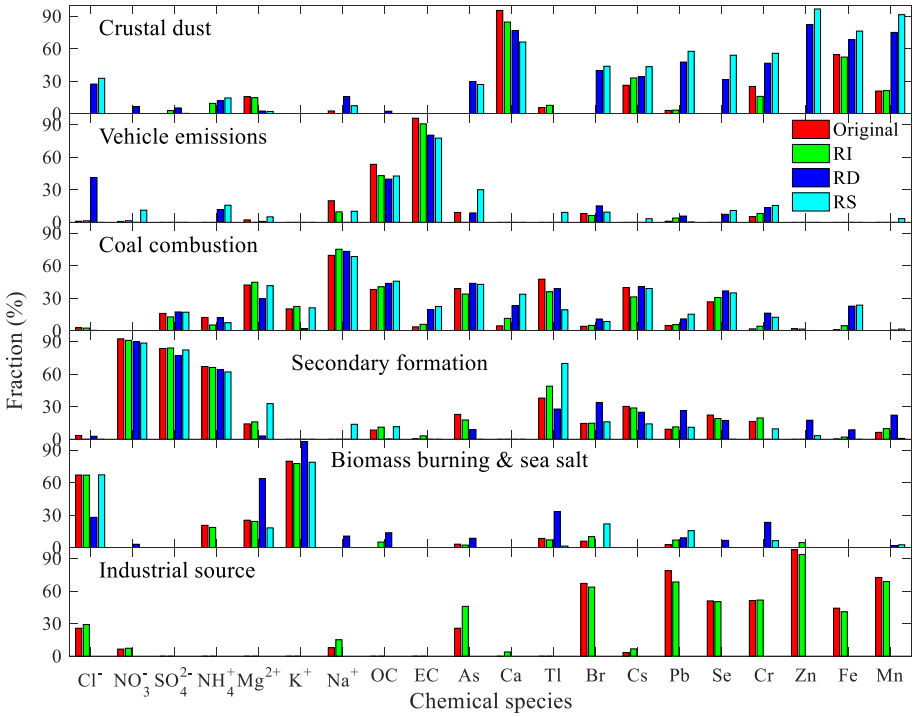

Figure 5 The influence of different TS components on source determination (Tianjin site). The industrial source was not identified from the RD and RS datasets. RBL dataset was investigated by PCA analysis instead of ME-2 due to the dataset has some negative values.

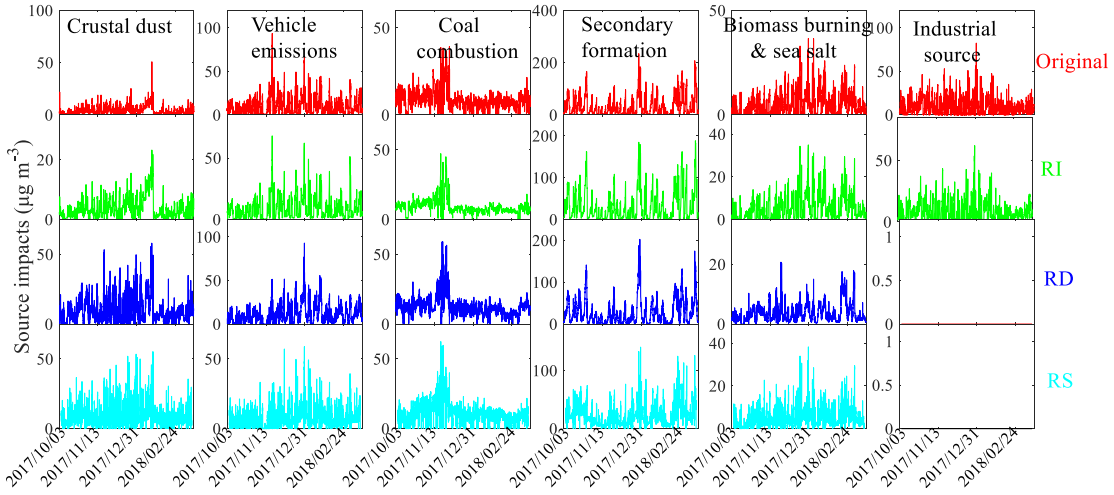

Figure 6 Source contributions to $PM_{2.5}$ for each source (vertical columns) and each dataset (horizontal rows) (Tianjin site). The blanks mean that the source has not been identified.

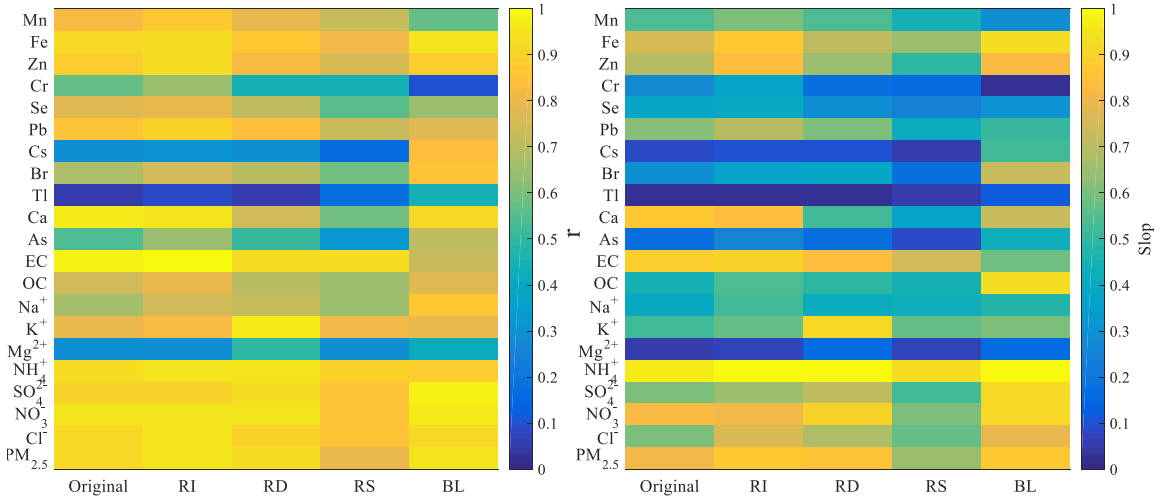

Figure S13. The performance of ME-2 from five datasets (Tianjin site). (Left): the slops between model and measured concentrations of chemical species and $PM_{2.5}$. (RI: intra-day removed dataset, RD: diurnal removed dataset, RS: synoptic removed dataset, BL: baseline dataset) (Right)The correlation coefficients between modeled and measured concentrations of chemical species and $PM_{2.5}$.

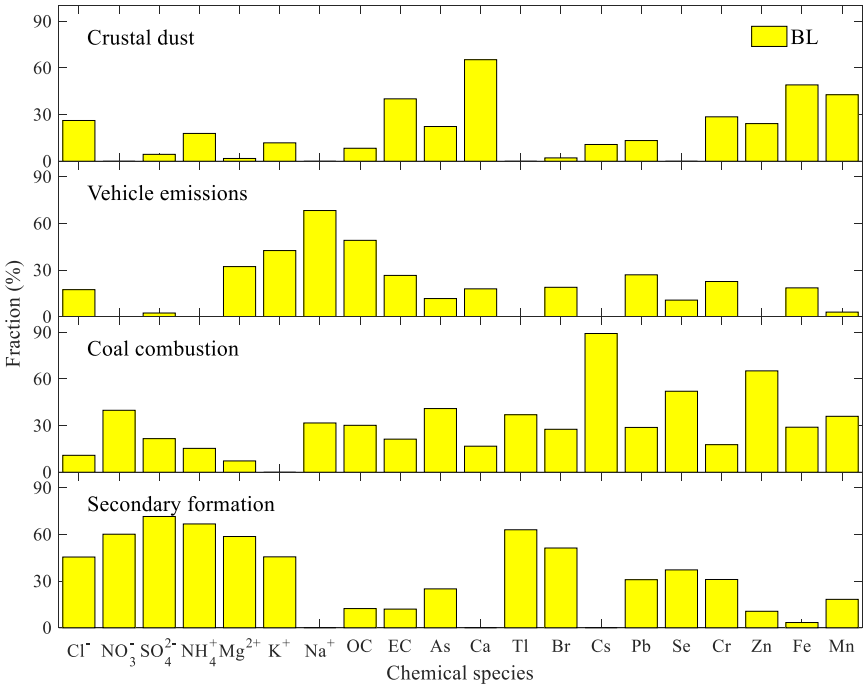

Figure S14. The factor profiles obtained from ME-2 from baseline dataset (Tianjin site).

Table 4. Average source contributions to $PM_{2.5}$ (μg m^{-3}) estimated by ME-2 from Tianjin for the original, RI, RD, and RS datasets during the entire sampling period.

		Crustal dust	Vehicle emission	Coal combustion	Biomass burning & sea salt	Industrial source	TPS[a]	Secondary formation (TSS[b])
During the entire sampling period	Original	4.3[c] (6%)	10.2 (14%)	8.5 (12%)	5.0 (7%)	10.2 (14%)	**38.2 (54%)**	**32.5 (46%)**
	RI	3.8 (6%)	9.2 (13%)	8.9 (13%)	5.9 (9%)	8.6 (12%)	**36.5 (53%)**	**32.6 (47%)**
	RD	9 (14%)	10.9 (17%)	12.8 (20%)	3.5 (6%)		**36.2 (57%)**	**27.3 (43%)**
	RS	9.2 (16%)	8.0 (14%)	11.5 (20%)	5.1 (9%)		**33.8 (59%)**	**23.0 (41%)**
Fall[d]	Original	3.7 (6%)	8.7 (14%)	10.4 (16%)	3.0 (5%)	10.0 (16%)	35.8 (56%)	27.6 (44%)
	RI	2.8 (5%)	7.4 (12%)	11.2 (18%)	3.2 (5%)	8.9 (14%)	33.5 (55%)	27.9 (45%)
	RD	7.9 (14%)	6.4 (11%)	15.2 (27%)	2.9 (5%)		32.4 (58%)	23.7 (42%)
	RS	8.0 (15%)	5.6 (11%)	14.6 (28%)	3.7 (7%)		31.9 (61%)	20.5 (39%)
Winter	Original	4.1 (5%)	10.7 (14%)	7.6 (10%)	5.2 (7%)	9.5 (12%)	37.1 (49%)	39.0 (51%)
	RI	3.9 (5%)	10.2 (14%)	7.6 (10%)	6.3 (8%)	8.1 (11%)	36.0 (48%)	39.4 (52%)
	RD	8.9 (13%)	13.0 (19%)	11.6 (17%)	3.7 (5%)		37.1 (53%)	32.7 (47%)
	RS	9.7 (16%)	9.4 (16%)	9.2 (15%)	5.3 (9%)		33.6 (56%)	26.6 (44%)

[a]TPS is the total contributions of crustal dust, vehicle emissions, coal combustion, biomass burning & sea salt, and industrial source. [b]TSS is the total contributions of secondary formation and nitrate source. [c]The data in the parentheses and outside the parentheses are the absolute values of average source contribution (μg m^{-3}) and percentages of average source contribution (%), respectively. [d] Fall included October and November, and winter included December, January, February, and March (15 days).

Table S7. Relative contributions (%) of the different TS components to the total variance of chemical species concentrations (Tianjin site).

	Intra-day (%)	Diurnal (%)	Synoptic (%)	Baseline (%)
$PM_{2.5}$	6	**25**	**60**	9
Cl^-	12	**44**	**38**	6
NO_3^-	4	**23**	**68**	6
SO_4^{2-}	4	**25**	**59**	12
NH_4^+	3	**18**	**62**	17
Mg^{2+}	9	24	**40**	**27**
K^+	14	**32**	**44**	10
Na^+	6	9	**17**	**69**
OC	14	**34**	**48**	4
EC	10	**33**	**49**	8
As	**34**	**43**	21	2
Ca	**24**	20	**24**	**33**
Tl	**32**	7	2	**59**
Br	**26**	**53**	19	2
Cs	16	13	**18**	**53**
Pb	23	**39**	**33**	6
Se	28	**34**	**30**	8
Cr	**48**	**29**	14	9
Zn	**26**	**44**	23	6
Fe	27	**31**	**29**	13
Mn	**29**	**33**	**29**	9

Table S8. Average concentrations of $PM_{2.5}$ and chemical species for five datasets (Tianjin site).

	Original	RI	RD	RS	RBL
$PM_{2.5}$(μg m^{-3})	69.7	68.1	62.8	57.4	21.1
Cl^- (μg m^{-3})	3.8	3.6	3.1	3.1	1.7
NO_3^- (μg m^{-3})	14.3	13.9	12.1	9.5	7.5
SO_4^{2-}(μg m^{-3})	7.4	7.3	6.7	5.8	2.6
NH_4^+ (μg m^{-3})	13.9	13.7	12.9	11.6	3.6
Mg^{2+}(μg m^{-3})	0.05	0.05	0.04	0.04	0.01
K^+ (μg m^{-3})	0.9	0.9	0.8	0.8	0.3
Na^+ (μg m^{-3})	0.9	0.9	0.9	0.9	0.05
OC (μg m^{-3})	7.3	7.1	6.7	6.6	1.4
EC (μg m^{-3})	3.9	3.7	3.4	3.2	1.5
As (ng m^{-3})	5.7	4.5	4.4	4.5	3.8
Ca (ng m^{-3})	312.8	289.0	283.4	281.8	84.5
Tl (ng m^{-3})	2.8	2.1	2.6	2.7	0.9
Br (ng m^{-3})	33.0	28.5	26.0	27.0	17.9
Cs (ng m^{-3})	9.4	8.3	8.6	8.0	3.4
Pb (ng m^{-3})	63.4	57.1	53.4	52.7	27.4
Se (ng m^{-3})	6.1	5.0	4.8	4.8	3.8
Cr (ng m^{-3})	6.1	4.7	4.7	5.2	3.8
Zn (ng m^{-3})	270.7	235.4	211.5	222.9	145.1
Fe (ng m^{-3})	600.8	545.5	528.6	538.4	191.0
Mn (ng m^{-3})	42.9	36.3	33.6	33.2	26.1

Table S9. Correlation coefficients (3378 samples) between original and intra-day removed dataset, diurnal removed dataset, and synoptic removed dataset for source contributions (Tianjin site).

	RI	RD	RS
Crustal dust[a]	0.89**	0.69**	0.52**
Vehicle emission	0.96**	0.82**	0.76**
Coal combustion	0.88**	0.68**	0.59**
Secondary formation	0.99**	0.93**	0.75**
Biomass burning & sea salt	0.97**	0.74**	0.81**
Industrial source[b]	0.90**		

[a]Crustal dust from RD and RS datasets mixed with industrial source. [b]Only ME-2 from original and RI datasets identified the Industrial source. **Significant correlation at 0.01 level.

Table S10. The results obtained from PCA from RBL dataset (Tianjin site).

Components	Factor 1	Factor 2	Factor 3	Factor 4
Cl^-	0.33	0.20	**0.78**	0.23
NO_3^-	0.26	**0.82**	0.10	0.27
SO_4^{2-}	0.17	**0.82**	0.22	0.31
NH_4^+	0.26	**0.73**	0.34	0.28
Mg^{2+}	0.08	0.16	-0.10	**0.83**
K^+	0.21	0.26	0.32	0.77
Na^+	0.28	0.23	0.21	0.17
OC	0.13	0.24	0.40	**0.65**
EC	0.24	0.20	**0.61**	**0.51**
As	0.10	**0.62**	0.41	0.07
Ca	**0.75**	0.06	0.21	0.04
Tl	0.02	-0.17	0.04	0.04
Br	0.18	0.37	**0.70**	0.01
Cs	0.09	0.34	0.07	-0.10
Pb	0.39	0.43	**0.60**	0.21
Se	0.47	**0.57**	0.30	0.11
Cr	**0.73**	0.20	0.07	0.23
Zn	0.47	0.18	**0.71**	0.07
Fe	**0.85**	0.21	0.34	0.08
Mn	**0.80**	0.29	0.28	0.12
Variance contribution (%)	44.9	8.7	6.4	5.4

Table S11. Average source contributions to $PM_{2.5}$ (μg m^{-3}) estimated by ME-2 from the BL datasets (Tianjin site).

	Crustal dust	Vehicle emission	Coal combustion	TPS[a]	Secondary formation(TSS[b])
During the entire sampling period	7.3[c] (14%)	12.0 (23%)	10.4 (20%)	**29.6 (58%)**	**21.3 (42%)**
Fall	3.4 (7%)	12.8 (28%)	16.5 (36%)	**32.7 (71%)**	**13.3 (29%)**
Winter[d]	8 (15%)	9.4 (17%)	10.5 (19%)	**28 (51%)**	**26.4 (49%)**

[a]TPS is the total contributions of crustal dust, vehicle emissions, and coal combustion. [b]TSS is the contributions of secondary formation. [c]The data in the parentheses and outside the parentheses are the absolute values of average source contribution (μg m^{-3}) and percentages of average source contribution (%), respectively. [d]The winter included 15 days in March 2018.

c) ME2 is a powerful tool to estimate the sources of PM and required model input

is non-negative. PCA was only used to analyze RBL dataset as negative values (about 40%) of the RBL dataset and the limitation of ME2.

PMF/ME2 does not need source profiles as model input but require receptor data. It is possible that one factor includes multiple sources and combine other chemical components in the factor profile except for the source markers (Canepari et al., 2009; Lee et al., 2009). Given that coal combustion, vehicle emissions, and crustal dust are collinearity sources that have similar profiles (Shi et al., 2009; Shi et al., 2011; Zhang et al., 2013), and that the absence of marker species (Si, Al, etc.) in the source profiles increased their collinear and uncertainties (Peng et al., 2016), these lead to difficulties in completely separating the three sources. We identified vehicle emissions and coal combustion according to the criterion that OC and EC fraction in vehicle emissions are higher than the values in coal combustion. We also analyzed the correlations of time series between source contributions and gaseous pollutants (SO_2, NO, NO_2) and diurnal patterns of source contribution (Figure S8). Correlation analysis showed vehicle emission has a significant correlation, with NO (ranging from 0.1 to 0.3, $p<0.01$) and NO_2 (ranging from 0.2 to 0.3, $p<0.01$). Correlation between coal combustion and SO_2 ranged from 0.4 ($p<0.01$) to 0.6 ($p<0.01$), for the four datasets. For the results of the original dataset, vehicle emissions exhibited a relatively high contribution to $PM_{2.5}$ during the nighttime, suggesting that diesel vehicles appeared and emitted pollutants during the nighttime (Gao et al., 2016). Coal combustion showed a stable diurnal trend, and crustal dust has high contributions from 0:00 to 12:00. The diurnal pattern of secondary formation primarily dominated by nitrate that peaked in the early morning

and at nighttime (Xu et al., 2014). Source diurnal trends estimated from RI dataset similar with results from original dataset, implying the small influences of intra-day TS component on the source diurnal trends. For the results from RS dataset, secondary formation (sulfate source) presented a broad peak during the daytime and might link to photochemical processes of sulfate. For results from RD and BL datasets, it is an expected result that all of four sources did not show obvious diurnal trends after removing the diurnal TS component.

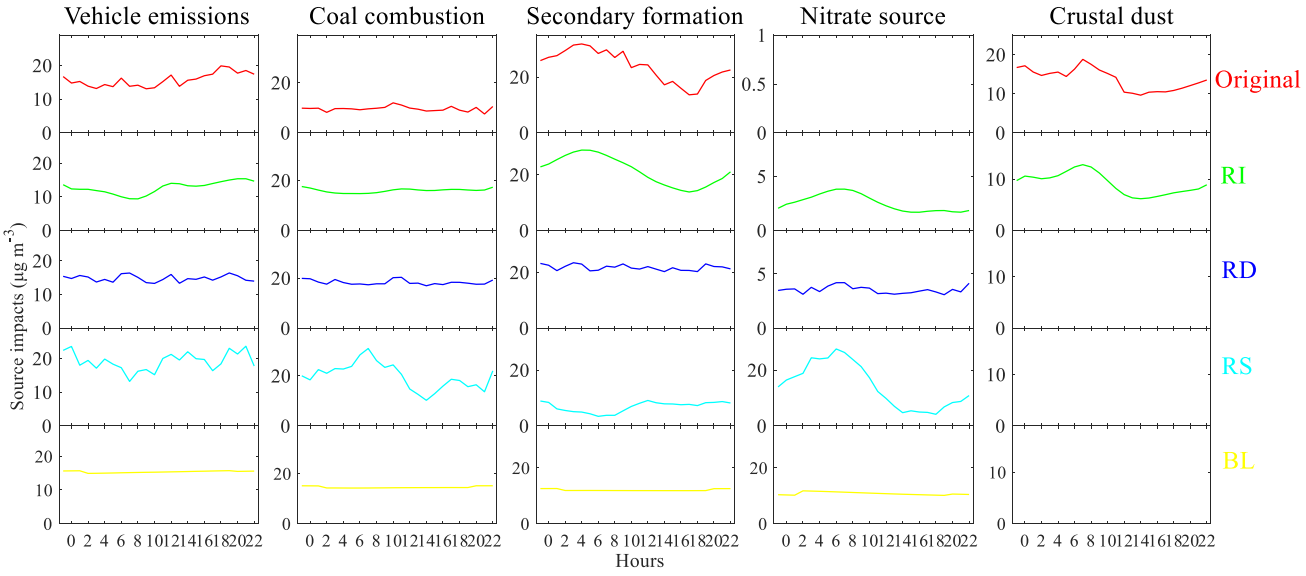

Figure S8. Diurnal trend of Source impacts for each source (vertical columns) and each dataset (horizontal rows) (Beijing site). The blanks mean that the source has not been identified.

References:

Canepari, S., Pietrodangelo, A., Perrino, C., Astolfi, M. L., Marzo, M. L.: Enhancement of source traceability of atmospheric PM by elemental chemical Fractionation. Atmos. Environ. 43, 4754-4765, doi: 10.1016/j.atmosenv.2008.09.059, 2009.

Gao, J., Peng, X., Chen, G., Xu, J., Shi, G. L., Zhang, Y. C., and Feng, Y. C.: Insights into the chemical characterization and sources of $PM_{2.5}$ in Beijing at a 1-h time resolution, Sci. Total. Environ., 542, 162-171, doi:

10.1016/j.scitotenv.2015.10.082, 2016.

Lee, D., Balachandran, S., Pachon, J., Shankaran, R., Lee, S., Mulholland, J. A., and Russell, A. G.: Ensemble-trained $PM_{2.5}$ source apportionment approach for health studies. Environ. Sci. Technol., 43(18), 7023-7031, doi: 10.1021/es9004703, 2009.

Peng, X., Shi, G. L., Gao, J., Liu, J. Y., Huangfu, Y. Q., Ma, T., Wang, H. T., Zhang, Y. C., Wang, H., Li, H., Ivey, C. E., and Feng, Y. C.: Characteristics and sensitivity analysis of multiple-time-resolved source patterns of $PM_{2.5}$, with real time data using Multilinear Engine 2, Atmos. Environ., 139, 113-121, doi: 10.1016/j.atmosenv.2016.05.032, 2016.

Shi, G. L., Xu, J., Peng, X., Xiao, Z. M., Chen, K., Tian, Y. Z., Guan, X. B., Feng, Y. C., Yu, H. F., Nenes, A., and Russell, A. G.: pH of aerosols in a polluted atmosphere: source contributions to highly acidic aerosol. Environ. Sci. Technol., 51, doi: 4289-4296, 10.1021/acs.est.6b05736, 2017.

Shi, G. L., Xu, J., Peng, X., Xiao, Z. M., Chen, K., Tian, Y. Z., Guan, X. B., Feng, Y. C., Yu, H. F., Nenes, A., and Russell, A. G.: pH of aerosols in a polluted atmosphere: source contributions to highly acidic aerosol. Environ. Sci. Technol., 51, doi: 4289-4296, 10.1021/acs.est.6b05736, 2017.

Shi, G. L., Zeng, F., Li, X., Feng, Y. C., Wang, Y. Q., Liu, G. X., and Zhu, T.: Estimated contributions and uncertainties of PCA/MLR–CMB results: Source apportionment for synthetic and ambient datasets. Atmos. Environ. 45, 2811-2819, doi: 10.1016/j.atmosenv.2011.03.007, 2011.

Monsalve, S. M., Martínez, L., Vásquez, K. Y., Orellana, S. A., Vergara, J. K., Mateo, M. M., Salazar, R. C., Salazar, R. C., and Lillo, D. D. C.: Trace element contents in fine particulate matter ($PM_{2.5}$) in urban school microenvironments near a contaminated beach with mine tailings, Chañaral, Chile. Environ. Geochem. Health., 40, 1077-1091, doi: 10.1007/s10653-017-9980-z, 2018.

Ojekunle, Z. O., Jinadu, O. O. E., Afolabi, T. A., and Taiwo, A. M.: Environmental Pollution and Related Hazards at Agbara Industrial Area, Ogun State. Sci. Rep., 8. doi :10.1038/s41598-018-24810-4, 2018.

Tian, Y. Z., Liu, J. Y., Han, S. Q., Shi, X. R., Shi, G. L., Xu, H., Yu, H. F., Zhang, Y. F., Feng, Y. C., and Russell, A. G.: Spatial, seasonal and diurnal patterns in physicochemical characteristics and sources of $PM_{2.5}$ in both inland and coastal regions within a megacity in China. J. Hazard. Mater., 342, 139-149, doi: 10.1016/j.jhazmat.2017.08.015, 2018.

Xu, J., Zhang, Q., Chen, M., Ge, X., Ren, J., and Qin, D.: Chemical composition, sources, processes of urban aerosols during summertime in northwest China, insights from high-resolution aerosol mass spectrometry. Atmos. Chem. Phys., 2014;14:12593-12611, doi.org/10.5194/acp-14-12593-2014, 2014.

Ye, H. J., Liao, X. F., Guo, S. L., Jiang, X. J., Yao, L., and Chen, X. S.: Development and Application of Continuous Atmospheric Heavy Metals Monitoring System Based on X-Ray Fluorescence, Adv. Mater., Res., 518-523, 1510-1515, doi: 10.4028/www.scientific.net/AMR.518-523.1510, 2012.

Zhang, J. Q., Peng, L., Bai, H. L., Liu, X. F., and Mu, L.: Source Apportionment of Particulate Matter Based on Carbon Isotope Mass Balance Model. Appl. Mech. Mater. 295-298, 1565-1569, doi: org/10.4028/www.scientific.net/AMM.295-298.1565, 2013.

Zhu, Y., Yang, L., Chen, J., Kawamura, K., Sato, M., Tilgner, A., van Pinxteren, D., Chen, Y., Xue, L., Wang, X., Simpson, I. J., Herrmann, H., Blake, D. R., and Wang, W.: Molecular distributions of dicarboxylic acids, oxocarboxylic acids and α-dicarbonyls in $PM_{2.5}$ collected at the top of Mt. Tai, North China, during the wheat burning season of 2014, Atmos. Chem. Phys., 18, 10741-10758, https://doi.org/10.5194/acp-18-10741-2018, 2018.